Heme binding by *Corynebacterium diphtheriae* HmuT: Function and heme environment

Supporting Information

Elizabeth H. Bennett,[†] Neval Akbas,[†] Seth A. Adrian,[§] Gudrun S. Lukat-Rodgers,[§] Daniel P. Collins,[‡] John H. Dawson, [‡] Courtni E. Allen,[Δ] Michael P. Schmitt, [Δ] Kenton R. Rodgers,[§,] and Dabney W. Dixon[†,*]*

[†]Department of Chemistry, Georgia State University, Atlanta, Georgia 30302-3965
[§]Department of Chemistry and Biochemistry, North Dakota State University, Fargo, North Dakota 58108-6050
[‡]Department of Chemistry and Biochemistry, University of South Carolina, Columbia, South Carolina 29208
[Δ]Laboratory of Respiratory and Special Pathogens, Division of Bacterial, Parasitic, and Allergenic Products, Center for Biologics Evaluation, and Research, Food and Drug Administration, Silver Spring, Maryland 20993

Figure S1. Alignment of the amino acid sequence of HmuT from various *Corynebacterium* species. Species are designated as follows: Cd: *C. diphtheriae* 1737/NCTC13129; CU: *C. ulcerans* 712; Cjk: *C. jeikeium* k411-jk0316; Cglut: *C. glutamicum* ATCC 13032; Curea: *C. urealyticum* DSM 7109. Conserved residues that were subjected to site-directed mutagenesis are indicated above the sequence alignment; asterisks indicate sequence identity and colons and periods show sequence similarity.

Figure S2. Alignment of the amino acid sequence of *Cd*HmuT with four HBPs with known crystal structures. Square boxes indicate the known axial ligands. Orange: *P. aeruginosa* PhuT (*1*) and *S. dysenteriae* ShuT (*1*). Green: *S. aureus* IsdE (*2*). Blue: *Y. pestis* HmuT (*3*). Red: *C. diphtheriae* HmuT. For *Cd*HmuT, M292 is also shown.

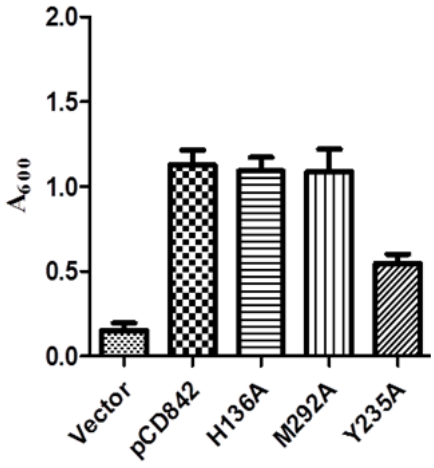

Figure S3. Hb-iron utilization assay. *C. ulcerans* CU77 (*hmuT*) carrying plasmids that encode the wild type (pCD842) and various mutants of the *hmuT* gene were assessed for their ability to use Hb as the sole iron source for growth in low-iron mPGT medium. Cultures were grown for 36 hours at 37 ^{o}C in the presence of 25 µg/ml Hb supplemented with 10 µM EDDA, and then cell density was measured by absorbance at A_{600}. Results are the mean of three independent experiments ± standard deviation. The growth difference between WT (pCD842) and Y235A is significant at $p < 0.01$.

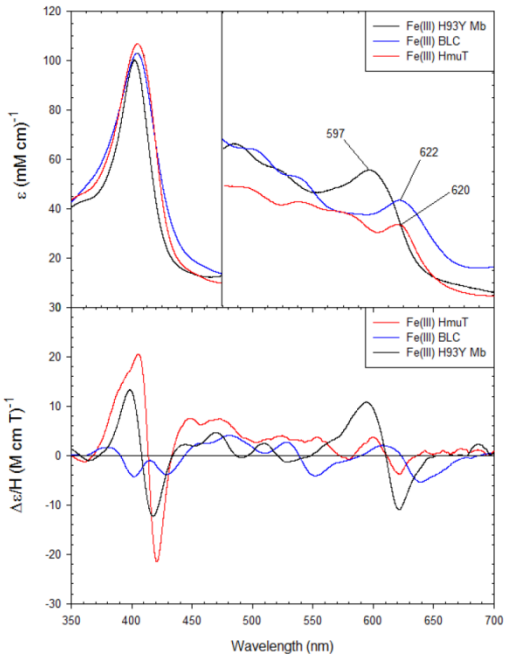

Figure S4. Comparison of the UV-visible absorption and MCD spectra for Fe(III) WT *Cd*HmuT at pH 6.5 with Fe(III) bovine liver catalase (BLC) and H93Y myoglobin. The samples were taken in 50 mM phosphate buffer. Spectra were slightly dependent on buffer conditions. The spectra of BLC and H93Y myoglobin were replotted from (*4-6*) and (*7*), respectively.

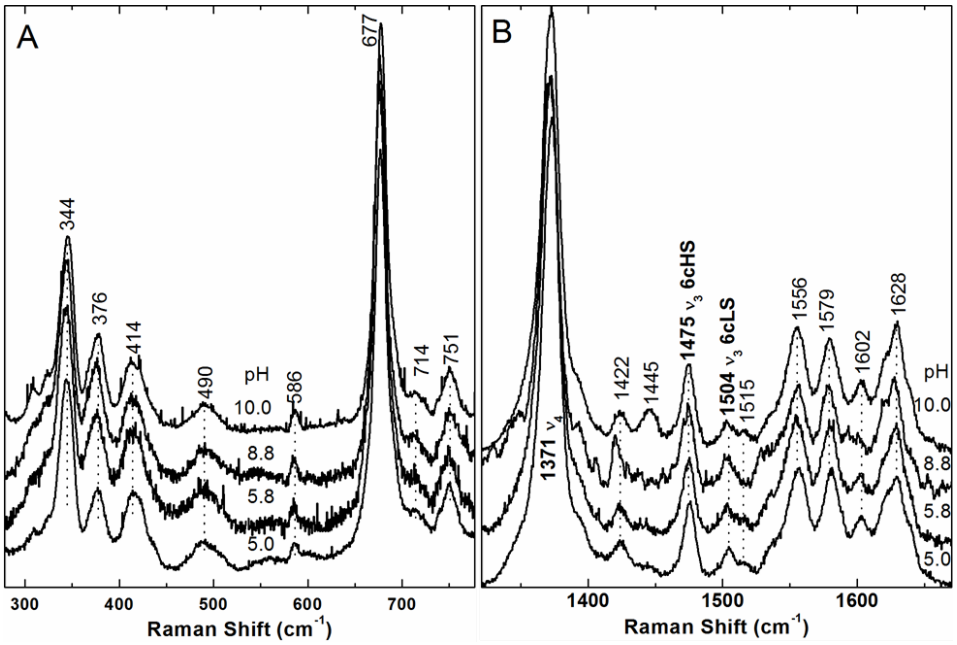

Figure S5. The rR spectrum of ferric WT *Cd*HmuT as a function of pH. A) Low frequency window. B) High frequency window. Protein concentration was 40 μM; excitation frequency of 413.1 nm was used with 9.4 mW laser power at the sample. The pH values are as indicated with the buffers described in the experimental section.

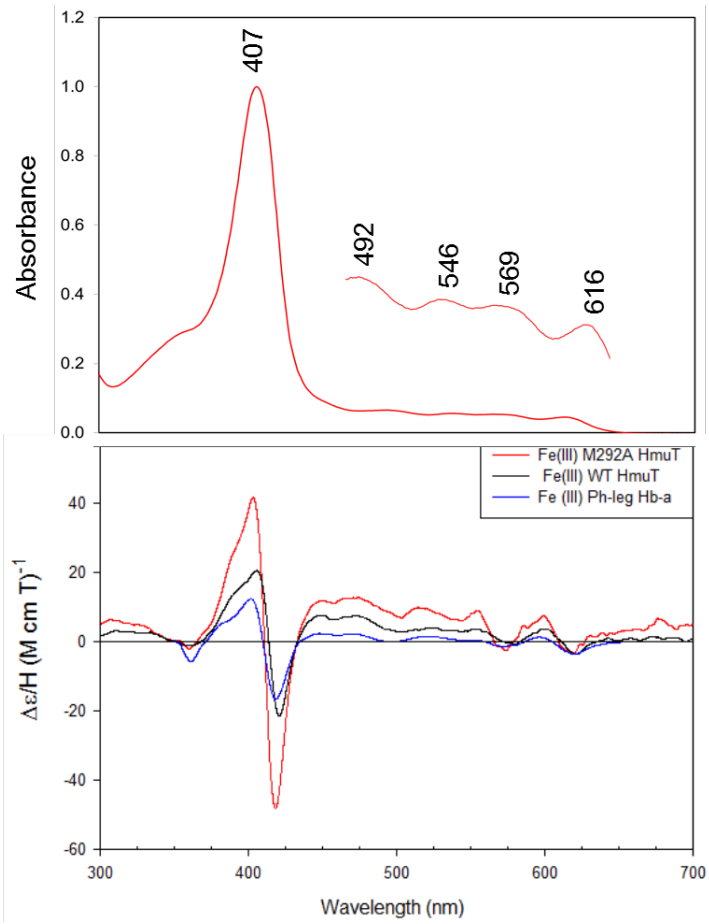

Figure S6. Top panel: UV-visible spectrum of M292A *Cd*HmuT. The sample was taken in 50 mM Tris-Cl, pH 7.0. Bottom panel: Comparison of the MCD spectra for Fe(III) M292A *Cd*HmuT at pH 6.5 with Fe(III) WT *Cd*HmuT and Fe(III) phenol-leg Hb *a*. The samples were taken in 50 mM phosphate buffer. The spectrum of phenol-leg Hb *a* was replotted from (*8*).

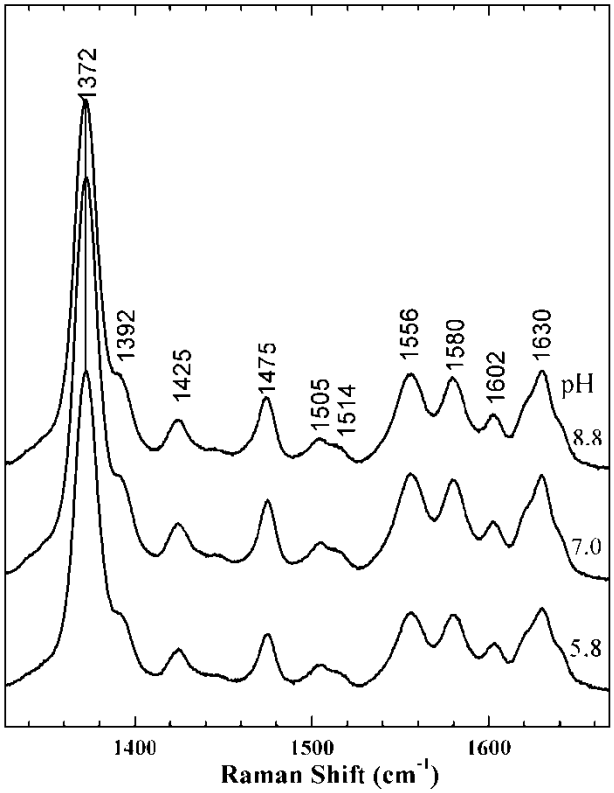

Figure S7. The rR spectrum of ferric M292A as a function of pH. Protein concentration was 36 μM; 406.7-nm excitation with 11 mW at the sample was used.

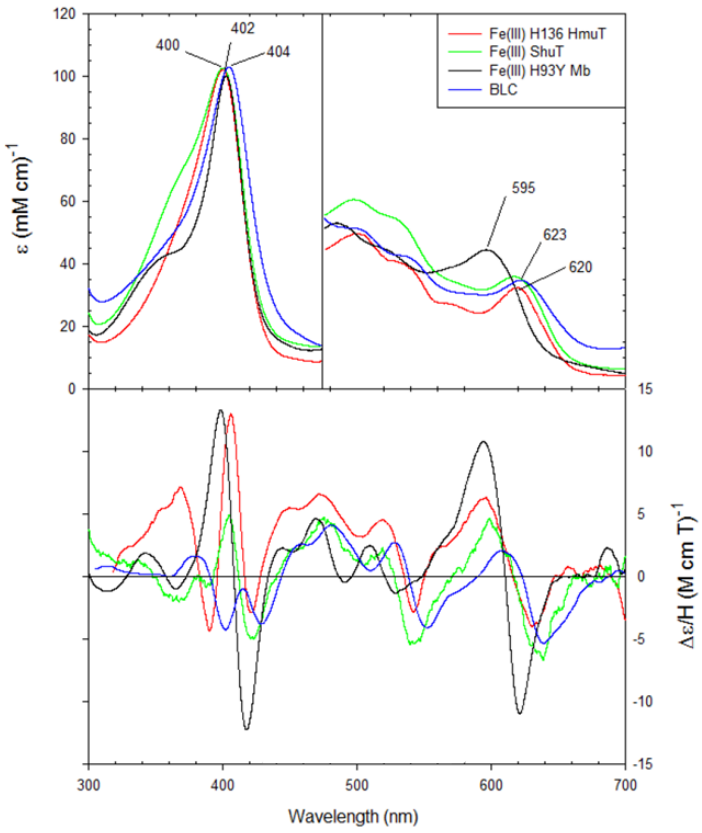

Figure S8. The UV-visible and MCD comparison spectra for Fe(III) H136A *Cd*HmuT at pH 6.5. Bottom panel: Comparison of the MCD spectra for Fe(III) H136A *Cd*HmuT with Fe(III) WT *Cd*HmuT, Fe(III) ShuT, Fe(III) H93Y Mb, and Fe(III) BLC. All samples in the work were taken in 50 mM phosphate buffer. Spectra of H93Y, ShuT, and BLC were replotted from (*7*),(*9*), and (*4*-*6*), respectively.

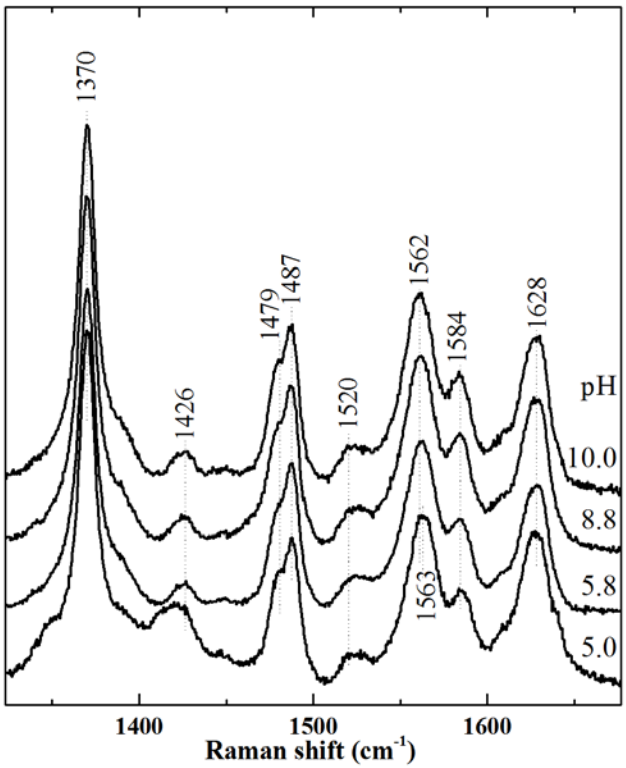

Figure S9. The rR spectrum of ferric H136A as a function of pH. Protein concentration was 25 μM; 406.7-nm excitation with 11 mW at the sample was used.

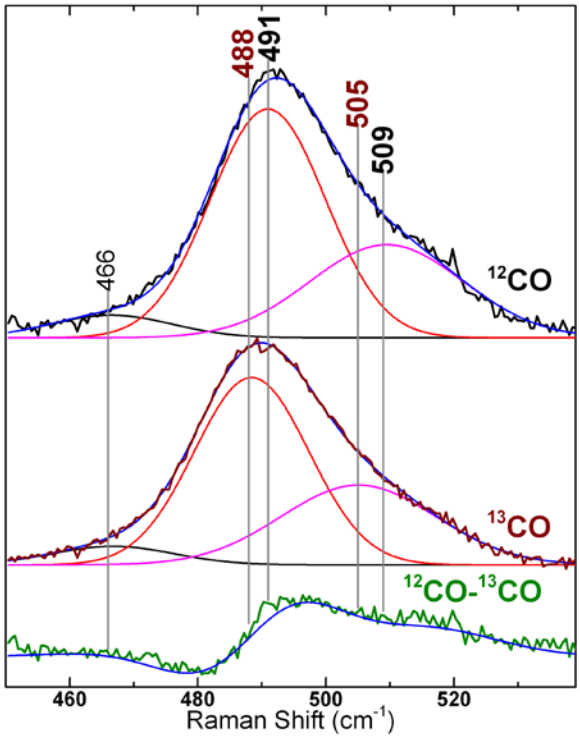

Figure S10. The Fe−C stretching region of the Y235A-CO rR spectrum. The experimental data for the natural abundance CO (black) and ^{13}CO (burgundy) complexes are shown with the peak fitting analysis of the 509/505 (magenta) and 491/488 cm^{-1} bands (red). Band widths are 24 and 18 cm^{-1}, respectively. The 466 cm^{-1} band is not ^{13}C sensitive. The simulated spectra are shown in blue; they are the sums of the fit peaks. The difference spectrum, obtained by subtraction of ^{13}CO spectrum from the natural abundance CO spectrum, is shown in green. The simulated ^{12}CO−^{13}CO difference spectrum (blue) is the difference between the simulated spectra for the ^{12}CO and ^{13}CO complexes.

Table S1. pK_a values of water *trans* to histidine in selected ferric heme proteins. The pK_a of ferrous microperoxidase 8 is reported as 10.9 (*10*).

Class	Protein	Fe(III)	Reference
CCOx	Cytochrome *c* oxidase	9.0	(*11*)
ClD	GR-1 chlorite dismutase	8.2	(*12*)
ClD	*Ideonella dechloratans* chlorite dismutase	8.5	(*13*)
ClD	*Dechloromonas aromatica* chlorite dismutase	8.7	(*14*)
FixL	*Rhizobium meliloti* FixL	9.3	(*15*)
FixL	*Bradyrhizobium japonicum* FixL	9.3	(*15*)
FixL	*Rhizobium meliloti* FixL	10	(*15*)
Hb	Leghemoglobin	8.3	(*16*)
Hb	Hemoglobin I (clam)	9.6	(*17*)
H-NOX	*Thermoanaerobacter tengcongensis* H-NOX	6.8	(*18*)
H-NOX	*Thermoanaerobacter tengcongensis* H-NOX I5L	7.9	(*18*)
H-NOX	*Thermoanaerobacter tengcongensis* H-NOX I5L/P115A	>10	(*18*)
H-NOX	*Thermoanaerobacter tengcongensis* H-NOX P115A	>10	(*18*)
HO	Heme oxygenase	7.6	(*19*;*20*)
HO	Mammalian HO-1	7.6	(*20*)
HO	Rat heme oxygenase-1	7.6	(*20*)
HO	*Pseudomonas aeruginosa* heme oxygenase	8.3	(*21*)
HO	Mammalian HO-2	8.5	(*22*)
HO	Bacterial heme oxygenase HmuO	9.0	(*23*)
HO	*Neisseriae meningitidis* heme oxygenase	9.3	(*24*)
HRP	Horseradish peroxidase	10.9	(*25*) (*26*)
IsdI	*Staphylococcus aureus* IsdI	7.1	(*27*)
Mb	Porcine myoglobin H64V/V68H/H93A/H97F	7.17	(*28*)
Mb	Aplysia myoglobin	7.6	(*25*)
Mb	Porcine myoglobin H64V/V68H/H93G/H97F	7.74	(*28*)
Mb	*Dolabella auricularia* myoglobin	7.8	(*29*)
Mb	Sperm whale myoglobin	8.95	(*25*)
MP	Microperoxidase 8	9.6	(*10*;*30*)

Table S2. Selected His/Tyr and Tyr heme-binding proteins with corresponding residues which are hydrogen-bonded to the axial tyrosine ligand.

Protein	Axial Ligation	Residue Hydrogen Bonding to the Axial Tyrosine	Motif[a]	Reference
S. aureus IsdA	Y166	Y170	Yxxx**Y**	(*31*)
S. aureus IsdB-N2	Y440	Y444	Yxxx**Y**	(*32*)
S. aureus IsdC	Y132	Y136	Yxxx**Y**	(*33*)
S. aureus IsdH-N3	Y642	Y646	Yxxx**Y**	(*34*)
B. anthracis IsdX1	Y136	Y140	Yxxx**Y**	(*35*)
B. anthracis IsdX2-N5	Y108	Y112	Yxxx**Y**	(*36*)
P. aeruginosa HasA	H32/Y75	H83	Yxxxxxxx**H**	(*37*)
S. marcesans HasA	H32/Y75	H83	Yxxxxxxx**H**	(*38*)
Y. pestis HasA	Y75	H81	Yxxxxx**H**	(*39*)
M. tuberculosis Rv0203	Y59/ H89	H63	Yxxx**H**	(*40*)
Y. pestis HmuT	Y70/H167	R72[b]	Yx**R**	(*3*)
P. aeruginosa PhuT	Y71	R73	Yx**R**	(*1*)
S. dysenteriae ShuT	Y67	K69[b]	Yx**K**	(*1*)
P. homomalla cAOS	Y353	R349	**R**xxxY	(*6*)
Human catalase	Y358	R354	**R**xxxY	(*41*)
M. avium ssp. *paratuberculosis* MAP	Y294	R290	**R**xxxY	(*6*)

[a] Residues in bold represent the amino acid hydrogen bonded to the axial ligand.

[b] Predicted that the residue could hydrogen bond the axial ligand, but is not directly observed in the crystal structure.

References

1. Ho, W. W., Li, H. Y., Eakanunkul, S., Tong, Y., Wilks, A., Guo, M. L., and Poulos, T. L. (2007) Holo-and apo-bound structures of bacterial periplasmic heme-binding proteins. *J. Biol. Chem. 282,* 35796-35802.

2. Grigg, J. C., Vermeiren, C. L., Heinrichs, D. E., and Murphy, M. E. (2007) Heme coordination by *Staphylococcus aureus* IsdE. *J. Biol. Chem. 282*, 28815-28822.

3. Mattle, D., Zeltina, A., Woo, J. S., Goetz, B. A., and Locher, K. P. (2010) Two stacked heme molecules in the binding pocket of the periplasmic heme-binding protein HmuT from *Yersinia pestis*. *J. Mol. Biol. 404*, 220-231.

4. Browett, W. R. and Stillman, M. J. (1979) Magnetic circular dichroism studies of bovine liver catalase. *Biochim. Biophys. Acta 577*, 291-306.

5. Abraham, B. D., Sono, M., Boutaud, O., Shriner, A., Dawson, J. H., Brash, A. R., and Gaffney, B. J. (2001) Characterization of the coral allene oxide synthase active site with UV-visible absorption, magnetic circular dichroism, and electron paramagnetic resonance spectroscopy: Evidence for tyrosinate ligation to the ferric enzyme heme iron. *Biochemistry 40*, 2251-2259.

6. Bandara, D. M. I., Sono, M., Bruce, G. S., Brash, A. R., and Dawson, J. H. (2011) Coordination modes of tyrosinate-ligated catalase-type heme enzymes: Magnetic circular dichroism studies of *Plexaura homomalla* allene oxide synthase, *Mycobacterium avium* ssp. paratuberculosis protein-2744c, and bovine liver catalase in their ferric and ferrous states. *J. Inorg. Biochem. 105,* 1786-1794.

7. Pond, A. E., Roach, M. P., Sono, M., Rux, A. H., Franzen, S., Hu, R., Thomas, M. R., Wilks, A., Dou, Y., Ikeda-Saito, M., Ortiz de Montellano, P. R., Woodruff, W. H., Boxer, S. G., and Dawson, J. H. (1999) Assignment of the heme axial ligand(s) for the ferric myoglobin (H93G) and heme oxygenase (H25A) cavity mutants as oxygen donors using magnetic circular dichroism. *Biochemistry 38*, 7601-7608.

8. Sievers, G., Gadsby, P. M., Peterson, J., and Thomson, A. J. (1983) Magnetic circular dichroism spectra of soybean leghaemoglobin *a* at room temperature and 4.2 K. *Biochim. Biophys. Acta 742*, 637-647.

9. Eakanunkul, S., Lukat-Rodgers, G. S., Sumithran, S., Ghosh, A., Rodgers, K. R., Dawson, J. H., and Wilks, A. (2005) Characterization of the periplasmic heme-binding protein ShuT from the heme uptake system of *Shigella dysenteriae*. *Biochemistry 44*, 13179-13191.

10. Vashi, P. R. and Marques, H. M. (2004) The coordination of imidazole and substituted pyridines by the hemeoctapeptide N-acetyl-ferromicroperoxidase-8 (Fe(II)NAcMP8). *J. Inorg. Biochem. 98*, 1471-1482.

11. Branden, M., Namslauer, A., Hansson, O., Aasa, R., and Brzezinski, P. (2003) Water-hydroxide exchange reactions at the catalytic site of heme-copper oxidases. *Biochemistry 42*, 13178-13184.

12. Hagedoorn, P. L., de Geus, D. C., and Hagen, W. R. (2002) Spectroscopic characterization and ligand-binding properties of chlorite dismutase from the chlorate respiring bacterial strain GR-1. *Eur. J. Biochem. 269*, 4905-4911.

13. Stenklo, K., Thorell, H. D., Bergius, H., Aasa, R., and Nilsson, T. (2001) Chlorite dismutase from *Ideonella dechloratans*. *J. Biol. Inorg. Chem. 6*, 601-607.

14. Streit, B. R., Blanc, B., Lukat-Rodgers, G. S., Rodgers, K. R., and Dubois, J. L. (2010) How active-site protonation state influences the reactivity and ligation of the heme in chlorite dismutase. *J. Am. Chem. Soc. 132*, 5711-5724.

15. Gilles-Gonzalez, M. A., Gonzalez, G., Perutz, M. F., Kiger, L., Marden, M. C., and Poyart, C. (1994) Heme-based sensors, exemplified by the kinase FixL, are a new class of heme protein with distinctive ligand binding and autoxidation. *Biochemistry 33*, 8067-8073.

16. Jones, D. K., Badii, R., Rosell, F. I., and Lloyd, E. (1998) Bacterial expression and spectroscopic characterization of soybean leghaemoglobin *a*. *Biochem. J. 330*, 983-988.

17. Kraus, D. W., Wittenberg, J. B., Lu, J. F., and Peisach, J. (1990) Hemoglobins of the *Lucina pectinata*/bacteria symbiosis. II. An electron paramagnetic resonance and optical spectral study of the ferric proteins. *J. Biol. Chem. 265*, 16054-16059.

18. Olea, C., Kuriyan, J., and Marletta, M. A. (2010) Modulating heme redox potential through protein-induced porphyrin distortion. *J. Am. Chem. Soc. 132*, 12794-12795.

19. Sun, J., Wilks, A., Demontellano, P. R. O., and Loehr, T. M. (1993) Resonance Raman and EPR spectroscopic studies on heme-heme oxygenase complexes. *Biochemistry 32*, 14151-14157.

20. Takahashi, S., Wang, J. L., Rousseau, D. L., Ishikawa, K., Yoshida, T., Host, J. R., and Ikedasaito, M. (1994) Heme-heme oxygenase complex structure of the catalytic site and its implication for oxygen activation. *J. Biol. Chem. 269*, 1010-1014.

21. Caignan, G. A., Deshmukh, R., Zeng, Y. H., Wilks, A., Bunce, R. A., and Rivera, M. (2003) The hydroxide complex of *Pseudomonas aeruginosa* heme oxygenase as a model of the low-spin iron(III) hydroperoxide intermediate in heme catabolism: C-13 NMR spectroscopic studies suggest the active participation of the heme in macrocycle hydroxylation. *J. Am. Chem. Soc. 125*, 11842-11852.

22. Ishikawa, K., Takeuchi, N., Takahashi, S., Matera, K. M., Sato, M., Shibahara, S., Rousseau, D. L., Ikedasaito, M., and Yoshida, T. (1995) Heme oxygenase-2 - Properties of the heme complex of the purified tryptic fragment of recombinant human heme oxygenase-2. *J. Biol. Chem. 270*, 6345-6350.

23. Chu, G. C., Tomita, T., Sonnichsen, F. D., Yoshida, T., and Ikeda-Saito, M. (1999) The heme complex of Hmu O, a bacterial heme degradation enzyme from *Corynebacterium diphtheriae* - Structure of the catalytic site. *J. Biol. Chem. 274*, 24490-24496.

24. Zeng, Y. H., Caignan, G. A., Bunce, R. A., Rodriguez, J. C., Wilks, A., and Rivera, M. (2005) Azide-inhibited bacterial heme oxygenases exhibit an S=3/2 (d(xz),d(yz))(3) (d(xy))(1)(d(z)(2))(1) spin state: Mechanistic implications for heme oxidation. *J. Am. Chem. Soc. 127*, 9794-9807.

25. Brunori, M., Amiconi, G., Antonini, E., Wyman, J., Zito, R., and Fanelli, R. (1968) Transition between acid and alkaline ferric heme proteins. *Biochim. Biophys. Acta 154*, 315-&.

26. Sitter, A. J., Shifflett, J. R., and Terner, J. (1988) Resonance Raman spectroscopic evidence for heme iron-hydroxide ligation in peroxidase alkaline forms. *J. Biol. Chem. 263*, 13032-13038.

27. Takayama, S. J., Ukpabi, G., Murphy, M. E. P., and Mauk, A. G. (2011) Electronic properties of the highly ruffled heme bound to the heme degrading enzyme IsdI. *Proc. Natl. Acad. Sci. USA 108*, 13071-13076.

28. Uno, T., Sakamoto, R., Tomisugi, Y., Ishikawa, Y., and Wilkinson, A. J. (2003) Inversion of axial coordination in myoglobin to create a "proximal" ligand binding pocket. *Biochemistry 42*, 10191-10199.

29. Yamamoto, Y., Chûjô, R., Inoue, Y., and Suzuki, T. (1992) Kinetic characterization of the acid-alkaline transition in *Dolabella auricularia* ferric myoglobin using ^{1}H-NMR saturation transfer experiments. *FEBS Lett. 310*, 71-74.

30. Munro, O. Q. and Marques, H. M. (1996) Heme-peptide models for hemoproteins. 2. N-acetylmicroperoxidase-8 - study of the pi-pi dimers formed at high ionic-strength using a modified version of molecular exciton theory. *Inorg. Chem. 35*, 3768-3779.

31. Grigg, J. C., Vermeiren, C. L., Heinrichs, D. E., and Murphy, M. E. P. (2007) Haem recognition by a *Staphylococcus aureus* NEAT domain. *Mol. Microbiol. 63*, 139-149.

32. Gaudin, C. F., Grigg, J. C., Arrieta, A. L., and Murphy, M. E. (2011) Unique heme-iron coordination by the hemoglobin receptor IsdB of *Staphylococcus aureus*. *Biochemistry 50*, 5443-5452.

33. Sharp, K. H., Schneider, S., Cockayne, A., and Paoli, M. (2007) Crystal structure of the heme-IsdC complex, the central conduit of the Isd iron/heme uptake system in *Staphylococcus aureus*. *J. Biol. Chem. 282*, 10625-10631.

34. Watanabe, M., Tanaka, Y., Suenaga, A., Kuroda, M., Yao, M., Watanabe, N., Arisaka, F., Ohta, T., Tanaka, I., and Tsumoto, K. (2008) Structural basis for multimeric heme complexation through a specific protein-heme interaction - The case of the third NEAT domain of IsdH from *Staphylococcus aureus*. *J. Biol. Chem. 283*, 28649-28659.

35. Ekworomadu, M. T., Poor, C. B., Owens, C. P., Balderas, M. A., Fabian, M., Olson, J. S., Murphy, F., Balkabasi, E., Honsa, E. S., He, C., Goulding, C. W., and Maresso, A. W. (2012) Differential function of Lip residues in the mechanism and biology of an anthrax hemophore. *PLoS Path. 8*.

36. Honsa, E. S., Owens, C. P., Goulding, C. W., and Maresso, A. W. (2013) The near-iron transporter (NEAT) domains of the anthrax hemophore IsdX2 require a critical glutamine to extract heme from methemoglobin. *J. Biol. Chem. 288*, 8479-8490.

37. Alontaga, A. Y., Rodriguez, J. C., Schonbrunn, E., Becker, A., Funke, T., Yukl, E. T., Hayashi, T., Stobaugh, J., Monne-Loccoz, P., and Rivera, M. (2009) Structural characterization of the hemophore HasAp from *Pseudomonas aeruginosa*: NMR spectroscopy reveals protein-protein interactions between holo-HasAp and hemoglobin. *Biochemistry 48*, 96-109.

38. Arnoux, P., Haser, R., Izadi, N., Lecroisey, A., Delepierre, M., Wandersman, C., and Czjzek, M. (1999) The crystal structure of HasA, a hemophore secreted by *Serratia marcescens*. *Nature Struct. Biol. 6*, 516-520.

39. Kumar, R., Lovell, S., Matsumura, H., Battaile, K. P., Moenne-Loccoz, P., and Rivera, M. (2013) The hemophore HasA from *Yersinia pestis* ($HasA_{yp}$) coordinates hemin with a single residue, Tyr75, and with minimal conformational change. *Biochemistry 52*, 2705-2707.

40. Owens, C. P., Du, J., Dawson, J. H., and Goulding, C. W. (2012) Characterization of heme ligation properties of Rv0203, a secreted heme binding protein involved in *Mycobacterium tuberculosis* heme uptake. *Biochemistry 51*, 1518-1531.

41. Putnam, C. D., Arvai, A. S., Bourne, Y., and Tainer, J. A. (2000) Active and inhibited human catalase structures: Ligand and NADPH binding and catalytic mechanism. *J. Mol. Biol. 296*, 295-309.